

ORGANIC PHOTONICS

https://doi.org/10.1070/QEL16758

Optical and photoelectric properties of multichromic cyanine dye J-aggregates

B.I. Shapiro, A.D. Nekrasov, E.V. Manulik, V.S. Krivobok, V.S. Lebedev

Abstract. **We report the results of investigation of spectra and kinetics of photoluminescence as well as of photoabsorption and photoelectric properties for multichromic molecular crystals consisting of J-aggregates of three cyanine dyes with various structures. An original 'self-assembly' method is used for fabricating such prolate ordered structures with a thickness of 5–100 nm, width of 0.1–5 μm, and length of 50–300 μm. The method is based on the formation of the anionic platform in a water solution, which absorbs light in the blue spectrum range and comprises J-aggregates of magnesium complexes of anionic cyanine dye. Then the 'matrix synthesis' is used for coating its surface with J-aggregates of the two cationic dyes that have the absorption maxima in the green and red spectral ranges. It is shown that each of the multichromic organic crystals produced in this way is a multilayer photoelement, which possesses photoconductivity in three excitonic absorption maxima (in the blue, green, and red spectral ranges) with the external quantum efficiency varying from 2.7% to 6.1%. The results obtained provide a basis for technological development of highly-ordered molecular structures, which are promising for using in organic and hybrid photonics and optoelectronics including thin-film photo-converters operating in wide spectral ranges.**

Keywords: *organic photonics, optics of micro- and nanostructures, multichromic dye J-aggregates, molecular crystals, Frenkel exciton, photoabsorption and photoluminescence, organic photoelements.*

1. Introduction

The interest to studying optical properties of various micro- and nanostructures and developing new materials on their basis is associated with needs for creating a new element basis in photonics and optoelectronics. Actually, such investigations are aimed at developing and producing new-generation photonic and optoelectronic devices such as light emitting diodes [1, 2], solar cells [3, 4], nanolasers [5, 6], nanowaveguides [7, 8], and near-field optical probes [9–14] used for localising light fields on nanometre scales. Thus, fundamental investigations and developments in organic and hybrid photonics and optoelectronics are quite important. As is shown in a series of works, the employment of an organic component is promising in developing efficient and relatively inexpensive hybrid photonic and optoelectronic devices (for example, in light emitting diodes on quantum dots and nanoplates [15–18], solar photoelements [19, 20], photodetectors, chemical and biological sensors [21–23]). In this connection, optical and photoelectric properties of various organic semiconductors (electro-conducting polymers, organic dyes, charge-transfer complexes) are being actively studied. Of particular interest are cyanine dyes that differ from other dye classes by the maximal light absorption and ability to form highly organised aggregates and molecular crystals. Electronic excitations of separate molecules in ordered aggregates of cyanine dyes are collectivised forming Frenkel excitons. Molecular aggregates have unique optical properties including extremely high oscillator strength in the J-band transition, which absorption maximum is red shifted relative to that of monomer molecules [24–26]. In addition, cyanine dye aggregates possess a high quantum yield of generating photo-excited charge carriers [27]. These properties of cyanine dye aggregates determine their practical application as high-efficiency spectral sensitisers in classical photographic materials on silver halogenides [28].

In the last 10–15 years, cyanine dye molecular aggregates have been widely used as an organic component in metal-organic nanostructures of various compositions, shapes, and dimensions, which is promising for developing next-generation hybrid photonic and optoelectronic devices. In particular, there is a large number of experimental and theoretical works, which study spectral characteristics of two- and three-layer nanostructures consisting of a metallic core (Ag or Au) and the external shell of ordered dye molecular aggregates (see [29–35] and references therein). In a series of works, authors calculated spectra of two- and three-layer metal-organic nanospheres [36–40], nanospheroids and nanorods [41–45], nanostars [46], and dumbbell-like nanoparticles [42]. These works are devoted to studying the electromagnetic coupling between molecular Frenkel excitons and localised plasmons by an example of systems consisting of gold or silver nucleus and monochromic J-aggregates of various cyanine dyes as an external shell. Shapiro et al. [47] have also performed experimental and theoretical studies of the optical properties of the hybrid nanospheres and nanorods with a metallic core and an external shell formed either by J-aggregates or H-aggregates. Molecular J- and H-aggregates differ by the angle of molecular packing in the aggregate [24], which results in a substantial difference in the optical properties of these ordered molecular systems and hybrid micro- and nanostructures fabricated on their basis.

The main goal of the present work is studying spectral-kinetic and photoelectric properties of multilayer molecular crystals of cyanine dyes with various structures, which are actually multichromic systems and, consequently, can effi-

B.I. Shapiro, A.D. Nekrasov, E.V. Manulik Moscow Technological University (MIREA), prosp. Vernadskogo 78, 119571 Moscow, Russia; **V.S. Krivobok, V.S. Lebedev** P.N. Lebedev Physical Institute, Russian Academy of Sciences, Leninsky prosp. 53, 119991 Moscow, Russia; e-mail: vslebedev.mobile@gmail.com

Received 22 June 2018
Kvantovaya Elektronika **48** (9) 856–866 (2018)
Translated by N.A. Raspopov

ciently absorb light in several different spectral ranges simultaneously. A new 'self-assembly' method is developed and used for fabricating such crystals, which can be utilised as efficient light converters operating in a wide spectral range. The study of aggregation processes of anionic cyanine dyes in water solutions has shown that the aggregation is stimulated by multicharged cations of metals [48, 49]. In this case, metal-complex compounds are produced [50]. Thermodynamic studies of the assembly processes of anionic dyes under the action of multicharged cations [51] indicate a decrease in enthalpy and entropy with J-aggregation. In preliminary experiments it was shown that in water dispersions, J-aggregates of anionic cyanine dyes (in metal-complex forms as well) may have a negative electro-kinetic potential under certain conditions. In our works we suggested the method for matrix assembly of cationic dye J-aggregates on a surface of electrically negative J-aggregates; the latter may be in the form of metal-complexes of anionic dyes [51 – 53] as well.

In the present work, this became the starting point for stating the problem on 'matrix assembly' of monolayers of cationic dye J-aggregates on a surface of the negatively charged (anionic) 'platforms' consisting of J-aggregates of magnesium complexes of anionic dyes so that multichromic cationic-anionic J-aggregates are produced. Particular tasks of the present work are studying the character and main features of absorption and luminescence spectra of synthesised multichromic molecular crystals consisting of J-aggregates of three cyanine dyes, which possess three excitonic absorption maxima in the blue, green, and red spectral ranges. Photoelectric properties of these crystals are studied, as well as absorption and luminescence spectra of the anionic and cationic J-aggregates forming them are obtained and analysed.

The paper is organised as follows. Section 2 presents a brief description of objects under study and optical measurement technique. In Appendix, the method for synthesising multichromic dye J-aggregates is concisely stated. In Section 3 we present results of the experimental study of absorption and luminescence spectra for the monochromic magnesium complex J-aggregates, which form the platform for multichromic J-aggregates. Absorption and luminescence spectra of cationic dye J-aggregates are also presented. In addition, we study the luminenescence kinetics of J-aggregate anionic platforms of studied dyes under their excitation by femtosecond laser pulses. On this basis, the nature of high- and low-energy bands in the emission spectra of monochromic J-aggregates of investigated dyes is discussed. In Section 4, experimental data are given on the absorption and luminescence spectra of synthesised three-component systems, i.e. multichromic J-aggregates consisting of cationic dye J-aggregates and platforms of J-aggregates of magnesium complexes of anionic dyes. Section 5 addresses the fabrication methods and describes the main parameters of organic photoelements developed on the basis of synthesised multichromic J-aggregates. Main results are summarised in Conclusions.

2. Objects under study and experimental methods

Nano-architecture of the crystals synthesised in this work (multichromic J-aggregates) is illustrated in Fig. 1. Each of such multichromic J-aggregates is an elongated multilayer ordered system consisting of negatively charged platforms of J-aggregates of magnesium complexes of anionic cyanine dye (*1*), on the surfaces of which the 'self-assembly' of J-aggregates of two other cationic cyanine dyes (*2* and *3*) is executed. For fabricating the anionic platform, we used one of two anionic thiamonomethinecyanine dyes (K1 or K2), which absorb light in the blue spectral range. For cationic dyes we used oxatrimethinecyanine (K3) and thiatrimethinecyanine (K4), which absorb light in the green and red spectral ranges, respectively. Structural formulas and spectral characteristics of each of the four dyes are given in Table 1.

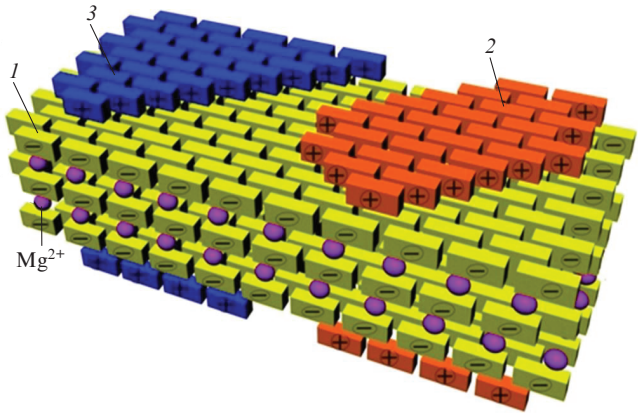

Figure 1. Photosensitive nano-architecture of a multichromic J-aggregate:
(*1*) metal-complex J-aggregate of anionic dye (K1 or K2); (*2*,*3*) J-aggregates of cationic dyes (K3 and K4).

Spectra of optical absorption and photoluminescence (PL) of multichromic J-aggregates in water nano-dispersions were measured in glass cells by an Ocean Optics USB2000+ spectrophotometer (USA) with a thermostabilised sample box and by a Cary Eclipse spectrofluorimeter (USA), respectively.

A schematic of the setup used for studying stationary photoluminescence of dye single micro-crystals is presented in Fig. 2. Micro-crystals (MCs) deposited on a glass were excited by radiation of a stationary semiconductor laser at a wavelength of 405 nm. The size of the excitation spot on a sample was ~ 3 mm at the exciting intensity of ~ 0.2 W cm^{-2}. An image of the PL spot magnified (2 – 20) by a microobjective (L2) and correcting lens (L1) was focused onto the entry slit of a grating spectrograph (Princeton Instruments Acton

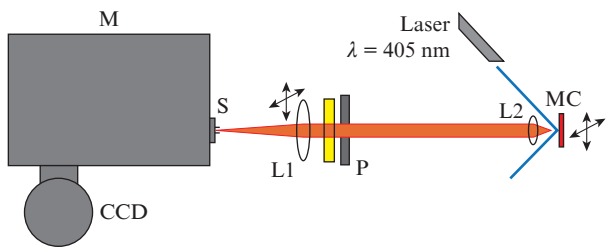

Figure 2. Schematic of the setup for studying dye microcrystal luminescence:
(MC) microcrystal under study; (L1) correcting lens; (L2) microobjective; (P) film polariser; (M) grating monochromator with a CCD-array; (S) input slit.

Table 1. Names and spectral characteristics of investigated monochromic cyanine dyes used for synthesising multichromic organic crystals. Letters denote various dye states: (M) monomer, (D) dimer, and (J) J-aggregate.

Dye number	Dye name and structural formula	Molar mass /g mol^{-1}	Molar extinction coefficient in alcohol /10^{-4} L mol^{-1} cm^{-1}	Position of the absorption maximum in water, λ_{max} /nm
K1	Triethylammonium salt of 3,3′-di(γ-sulfopropyl)-5,5′-dichlorothiamonomethincyanine 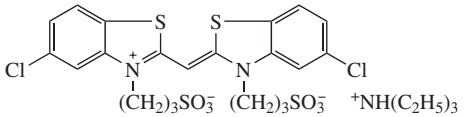	696.1	7.8	408 (D) 428 (M) 465 (J)
K2	Sodium salt of 3,3′-di(γ-sulfopropyl)-4, 5, 4′, 5′-dibenzothiamonomethincyanine 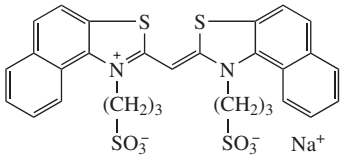	648.8	7.2	428 (D) 456 (M) 492 (J)
K3	Ethylsulfate of 3,3′-di(2-hydroxyethyl)-5,5′-diphenyl-9-ethyl-oxatrimethincyanine 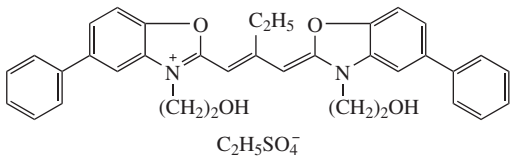	638.0	14.5	470 (D) 507 (M) 545 (J)
K4	Chloride of 3,3′-di(2-hydroxyethyl)-5,5′-dimethoxy-9-ethyl-thiatrimethincyanine 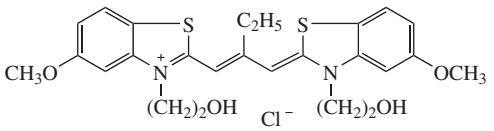	520.5	11.0	560 (D) 580 (M) 640 (J)

SP2500), which had the linear dispersion of 1.6 nm mm^{-1}. Scattered laser radiation was additionally reduced by a light filter transmitting radiation with wavelengths longer than 440 nm. The degree of light polarisation was measured by a film polariser placed between the microobjective and correcting lens. A liquid-nitrogen-cooled multichannel CCD-array was used as a radiation detector. The spatial resolution of the system was approximately 2 μm at the maximal magnification.

The recording system described is capable to analyse microcrystal photoluminescence in two regimes. In the first regime, the spectrograph grating operated in the zero diffraction order, and the slit width was 3 mm. Thus, a microphotograph of a luminescent fragment on the sample surface was recorded, and microcrystals were selected for the following analysis. After the microcrystal is chosen, its image is matched with a centre of the monochromator slit by lens L1. Photoluminescence spectra of the microcrystal chosen were analysed in another regime, where the grating was turned to the working position (the first diffraction order) and the entry slit was narrowed to 20 μm. Such a slit width in concordance with the CCD-matrix pixel size (20 μm) provides the spectral resolution no worse than 0.035 nm. In this case, the image on the photodetector corresponded to the 'spectral-spatial' picture of a photoluminescence signal. Hence, if the crystallite was oriented along the slit, it was possible to spatially analyse its luminescence in a single measurement cycle.

Photoluminescence kinetics was measured under the excitation by the second harmonic of a mode-locked Ti:Sapphire laser. The pulse duration was 2.5 ps at a pulse repetition frequency of 76 MHz. Data presented in this work are obtained under the excitation at wavelength $\lambda = 400$ nm ($\hbar\omega = 3.10$ eV). In all experiments, a diameter of the exciting radiation spot was ~100 μm. The spectral-temporal kinetics of the signal was detected by using a monochromator combined with a Hamamatsu C5680 streak-camera. The spectral and time resolution was 1.5 meV and 10 ps, respectively.

3. Spectral-kinetic properties of monochromic J-aggregates

3.1. Absorption and luminescence spectra of anionic dye solutions and monochromic J-aggregates of magnesium complexes of the dyes

As follows from photoabsorption spectra of the initial solutions of K1 and K2 dyes at a concentration of 2.5×10^{-5} M, they comprise the dyes in monomer and dimer forms and have no J-aggregates (Fig. 3). On the basis of anionic dyes K1 and K2, J-aggregates were synthesised in the form of magnesium complexes. Insertion of magnesium sulphate $MgSO_4$ at a concentration of 1×10^{-4} M to these solutions leads to formation of J-aggregate narrow excitonic absorption bands shifted to the long-wavelength spectral range relative to the bands of monomer and dimer forms of these dyes. Spectral investigations performed in this work show that these K1 and K2 J-aggregates have maxima of optical excitonic absorption

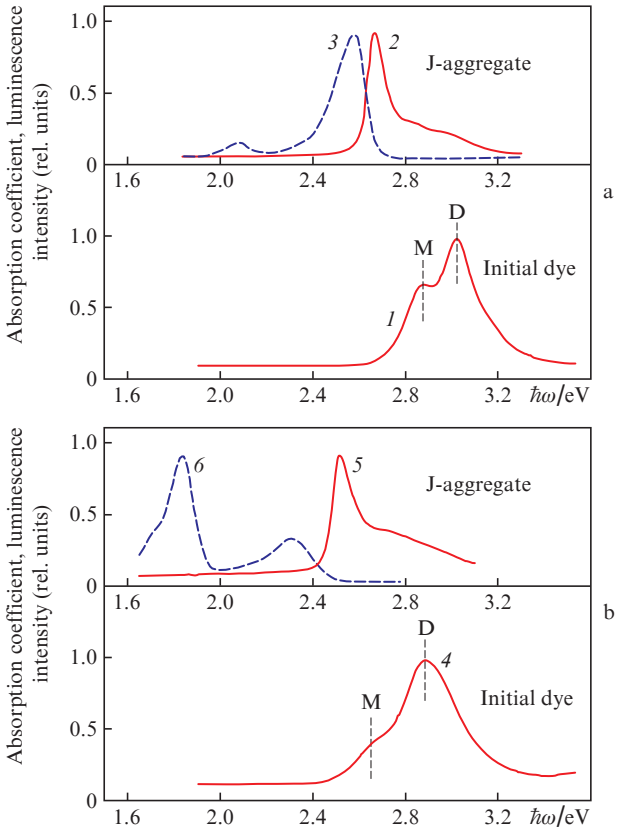

Figure 3. Normalised absorption spectra of initial water solutions of anionic K1 and K2 dyes with the concentration of 2.5×10^{-5} M [(*1*) and (*4*), respectively] and of water solutions comprising J-aggregates [(*2*) and (*5*), respectively] of magnesium complexes of these dyes. Letters M and D show positions of the peak absorption for monomers and dimers; *3* and *6* – photoluminescence spectra of solutions comprising J-aggregates of magnesium complexes of K1 and K2 dyes, respectively.

in the quantum energy ranges $\hbar\omega \approx 2.7$ and 2.5 eV, respectively (Fig. 3).

According to measurements of the electro-kinetic potential, J-aggregates of magnesium complexes K1 and K2 in a water medium have the negative ζ potential in the range from –10 to –42 mV, which is related to the exit of magnesium cations to a solution volume. Thus, J-aggregates of these complexes in a water medium are anionic platforms with a negative charge on the surface (due to the negative charge of sulfapropyl groups in dye molecules), which was used for the matrix assembly of cationic dye J-aggregates on their surfaces [54].

Curves (*3*) and (*6*) in Fig. 3 correspond to photoluminescence spectra of water solutions comprising synthesised J-aggregates of magnesium complexes of anionic dyes. One can see that the excitonic luminescence signal is maximal near a relatively weak long-wavelength wing of excitonic absorption. It means that the emission spectrum of J-aggregates is determined by low-frequency transitions corresponding to the 'tail' of the excitonic density of states. In addition to high-energy narrow bands of excitonic luminescence, an intensive photoluminescence line is detected in the low-energy part of the spectrum for each of the J-aggregates of magnesium complexes K1 and K2. Note that a position of the maximum of the low-energy luminescence band depends on the position of the excitonic absorption band maximum. The half-width of this band is small, which testifies similarity of types of the defects observed and the substantial influence of dye molecule structure and aggregate molecular structure on the nature of this luminescence band (for more details see Section 3.3).

In Fig. 4, one can see absorption and luminescence spectra of J-aggregates of cationic K3 and K4 dyes, which form excitonic absorption peaks in the range of photon energy $\hbar\omega \approx$ 2.3 and 1.9 eV, respectively. For J-aggregates of these dyes the picture is qualitatively similar to that in Fig. 3; the difference is that the absorption and luminescence bands are shifted toward the long-wavelength side. The relative intensities of luminescence maxima for J-aggregates of magnesium complexes K1 and K2 and for J-aggregates K3 and K4 are, respectively, 20 : 14 : 15 : 1.

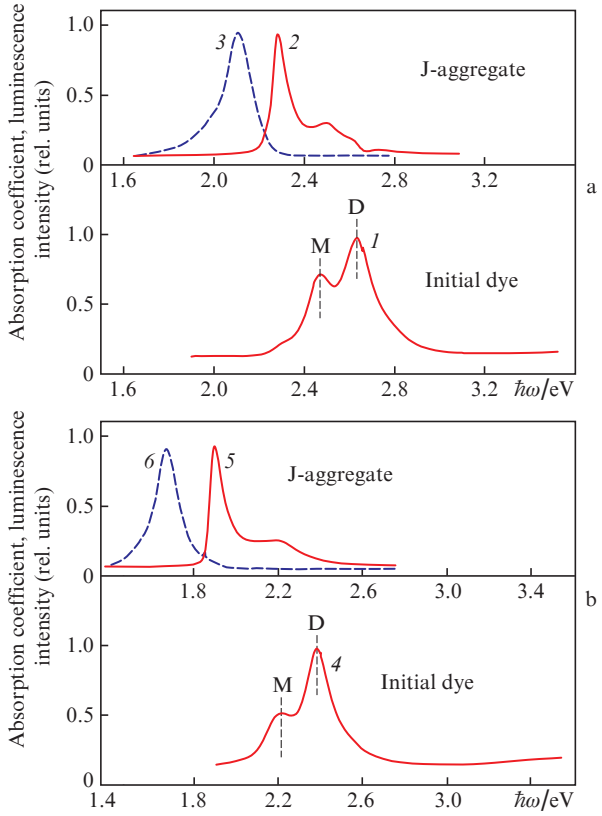

Figure 4. Normalised absorption spectra of initial water solutions of cationic K3 and K4 dyes with the concentration of 2.5×10^{-5} M [(*1*) and (*4*), respectively] and of water solutions comprising J-aggregates of these dyes [(*2*) and (*5*), respectively]. Letters M and D show positions of the peak absorption for monomers and dimers; (*3*) and (*6*) photoluminescence spectra of solutions comprising J-aggregates of K3 and K4 dyes, respectively.

Note that despite the relatively narrow photoabsorption peaks of separate monochromic J-aggregates, the resulting optical absorption spectra for synthesised multichromic J-aggregates of dyes (see Fig. 1), which possess three excitonic absorption maxima (in the blue, green, and red spectral ranges), totally cover the visible spectral range.

3.2. Photoluminescence of magnesium complexes of anionic dye J-aggregates

In investigations by the method of fluorescent microscopy it was established that microcrystals of J-aggregate magnesium complexes K1 and K2 obtained have a shape of long bars

('pales'). For example, a luminescent microphotograph is presented in Fig. 5 for a single monochromic J-aggregate crystal of the magnesium complex of dye K1. The images are obtained by the method described in Section 2 in the spectral range 0.45–0.90 μm on the installation shown schematically in Fig. 2. The maximal photoluminescence intensity is detected when the polariser is oriented in parallel to the long axis of the J-crystal along which the oriented growth of J-aggregate was realised. It means that the optical anisotropy of J-aggregates under study is tied to the axis of growth in a wide wavelength range, and J-aggregates mainly grow along the chromophore long axis of molecules of dyes included. This agrees with the data from [55].

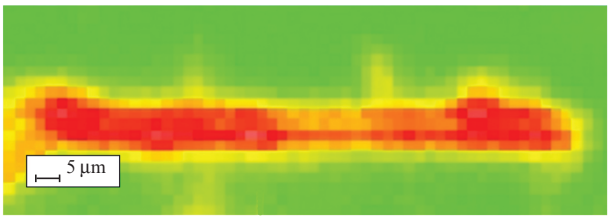

Figure 5. Microphotograph of the luminescence of a single crystal consisting of the J-aggregate of magnesium complexes of K1 dye.

According to the results of fluorescent optical microscopy, the dimensions of produced J-aggregates of magnesium complexes of anionic K1 and K2 dyes were, depending on particular synthesis conditions, as follows: the thickness was 5–100 nm, width was 0.1–5 μm, and length was 50–300 μm.

In Fig. 6 one can see characteristic luminescence spectra obtained for parallel and perpendicular signal polarisations relative to the long crystal axis (anionic platform of J-aggregates of the magnesium complex of dye K1). The modulation of the luminescence spectrum is, seemingly, explained by the interference due to light reflection from microcrystal faces. In the short-wavelength part of the spectra, this modulation is suppressed by noticeable light absorption near the resonance excitonic band. Note that along with the resonance excitonic luminescence of J-aggregates, the detected emission spectrum of single crystals has a long-wavelength band shifted to the red relative to the maximum of J-aggregate excitonic

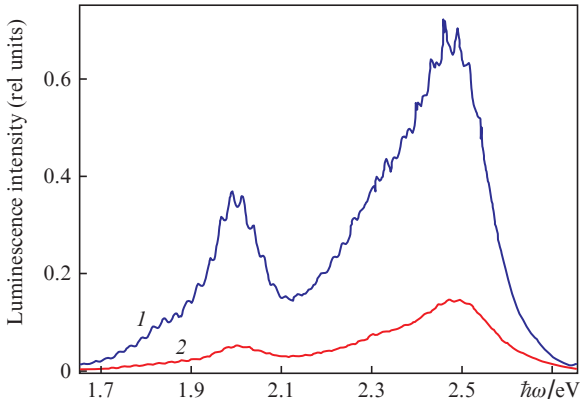

Figure 6. Luminescence spectra of a single J-aggregate of magnesium complexes of K1 dye in parallel (*1*) and perpendicular (*2*) polarisations relative to the crystal long axis.

absorption by approximately 0.45 eV. This band was already mentioned above for water solutions of J-aggregates of the magnesium complexes of K1 and K2 dyes. Its appearance in the case of a single (isolated) microcrystal proves relation between the low-energy (long-wavelength) luminescence maximum (in the range $\hbar\omega \approx 1.9$–2.1 eV) and electronic states of J-aggregates. The low-energy luminescence maximum is also specific in a noticeable degree of the linear polarisation with the same polarisation vector orientation as in the case of excitonic luminescence.

In the case of two luminescence bands, which demonstrate a noticeable linear polarisation of photoluminescence along the crystal growth axis, the tendency described above was observed for studied magnesium complex J-aggregates. Since the crystal growing axis coincides with the dye molecule orientation in the crystal one may assert that the luminescence in magnesium complex J-aggregates is determined by two main types of transitions, for which orientation of the dipole moment matrix element reproduces orientation of dye molecules.

3.3. Nature of bands in the luminescence spectrum of J-aggregates of anionic dyes

Measurements of luminescence spectra of J-aggregates of magnesium complexes of dyes K1 and K2 show that in addition to the high-energy maximum of resonance excitonic luminescence characterised by a relatively small red (Stokes)

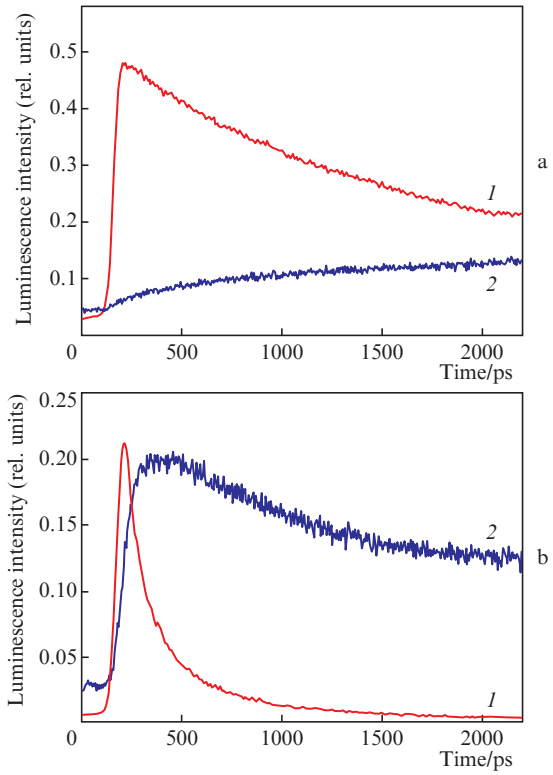

Figure 7. Luminescence kinetics of anionic platforms based on J-aggregates of dyes (a) K1 and (b) K2 for resonance excitonic (*1*) and long-wavelength (*2*) luminescence bands. For K1, the resonance excitonic luminescence corresponds to the photon energy of 2.43 eV and the long-wavelength luminescence corresponds to the photon energy of 2.02 eV. For K2, the resonance excitonic and long-wavelength luminescence correspond to the photon energies of 2.31 and 1.84 eV, respectively.

energy shift ($\hbar\omega \sim 0.05-0.1$ eV) relative to the maximum of J-aggregate excitonic absorption, there is a second (long-wavelength) maximum of luminescence, which exhibits a more substantial shift ($\hbar\omega = 0.4-0.5$ eV) to the low-energy spectral range.

Measurement results for kinetic photoluminescence of anionic platforms of J-aggregates K1 and K2 are shown in Fig. 7 under the conditions of exciting J-aggregates by femtosecond radiation pulses. From these data one may conclude that the characteristic decay times of resonance excitonic luminescence and luminescence with a large Stokes (red) shift are ~0.1 and 10 ns, respectively. The two-order difference in the decay times confirms a different nature of the short-wavelength luminescence peak (which is related to Frenkel excitons) and long-wavelength luminescence peak of synthesised multilayer dye aggregates. We should particularly emphasise the relatively slow kinetics of the initial growth of photoluminescence signal intensity in the low-energy bands. In particular, the maximal intensity of these bands is detected at substantially longer times than the peak intensity of resonance excitonic luminescence.

The scope of data presented above points to the fact that in anionic platforms of J-aggregates the luminescence with a large long-wavelength shift of the band maximum relative to the maximum of excitonic absorption is related to localised electronic states, which have sufficiently long lifetimes and, consequently, sufficiently low photorecombination probabilities as compared to those of resonance excitonic luminescence of J-aggregates.

In order to establish the nature of localised electron states responsible for the long-wavelength bands in emission spectra of anionic platforms we performed a series of experiments in which the influence of J-aggregate dimensions and growth regimes on their luminescence spectra was estimated. In particular, Fig. 8 presents spectra of optical absorption and luminescence for J-aggregates of the magnesium complexes of K1 dye in 5, 25, and 45 min after the synthesis. One can see that in the process of J-aggregate growing, the photoabsorption spectra slightly vary, whereas spectra of luminescence radically change. As the liquid nanocrystal dispersion of magnesium complex J-aggregates becomes settled, the luminescence intensity of the long-wavelength band around $\hbar\omega \approx 2.1$ eV falls whereas the narrow band of the resonance excitonic luminescence with the maximum in the region $\hbar\omega \approx 2.55$ eV grows. Probably, this is related to recrystallisation of small J-aggregates, which have a substantial quantity of surface defects, to high-ordered J-aggregates of a greater size with sparse defects (Ostwald ripening). Note that the part of the surface levels of microcrystals is small as compared to the total (combined) density of states; consequently, the former are weakly revealed in optical absorption spectra, which corresponds to the experimental data. Hence, results presented in Fig. 8 testify that variation of the duration of metal-complex J-aggregate synthesis makes it possible to obtain crystals with desirable dimensions and spectral-luminescence properties. In particular, one can control the luminescence intensity ratio for the resonance excitonic and long-wavelength bands.

Analysis of photoabsorption and luminescence spectra obtained for molecular crystals of J-aggregates of magnesium complexes K1 and K2 allows one to conclude that the low-energy luminescence maximum in the range 1.9–2.1 eV is related to defects in small J-aggregates, which play the role of excitonic traps. This is confirmed by the literature data

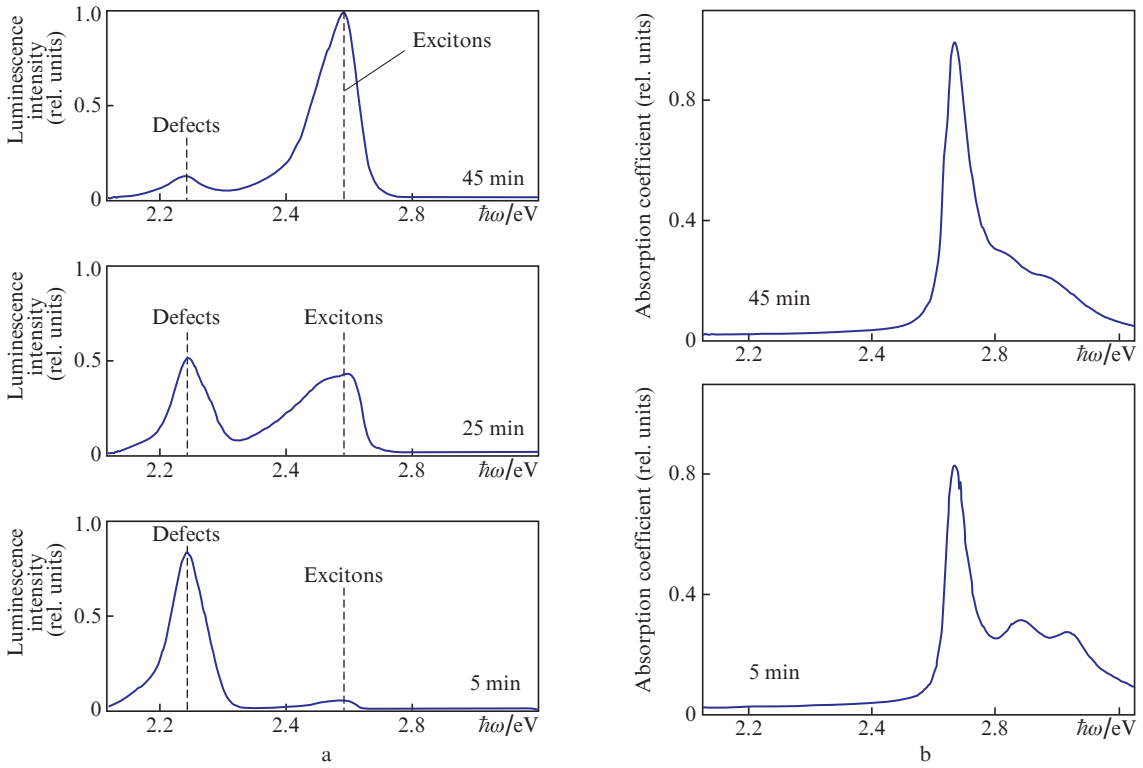

Figure 8. Normalised luminescence (a) and absorption (b) spectra of a water dispersion of magnesium complexes of K1 dye ($C_{D1} = 5 \times 10^{-5}$ M $C_{MgSO_4} = 1 \times 10^{-4}$ M) vs. time passed after the synthesis (shown in the figure). Luminescence is excited by UV radiation with the photon energy of 3.40 eV.

[56–67], according to which the additional maximum of J-aggregate luminescence that has a substantial Stokes shift relative to the maximum of excitonic absorption is explained by either packing defects of dye molecules in the molecular crystal lattice of J-aggregate, or defects on its surface. These defects are centres of photoluminescence because they can trap molecular Frenkel excitons migrating along the J-aggregate with subsequent photorecombination of electrons and holes in localised excitons.

Thus, experimental and literature data available allow us to suppose that the long-wavelength luminescence maximum with the Stokes shift of ~0.5 eV is mainly related to surface defects of small-size J-aggregates, which are either in a solution, or on a surface of growing J-aggregates. Note that in the molecular crystals studied, the processes of radiationless thermal (phonon) relaxation and exciton–phonon interaction play a substantial role.

4. Optical properties of multichromic J-aggregates

Absorption spectra of the triple systems of multichromic J-aggregates comprising J-aggregates of cationic K3 and K4 dyes and anionic platforms of magnesium complexes K1 and K2 are presented in Fig. 9. One can see that the synthesised multichromic systems comprising J-aggregates of three dyes have three intensive maxima of excitonic absorption in the blue, green, and red spectral ranges. The positions of these bands reproduce positions of the excitonic absorption peaks in the initial platforms with the accuracy of ~0.1 eV. It means that in multichromic J-aggregates, the main part of excitonic states preserves their properties to a certain degree.

Importantly, the positions of the excitonic absorption maxima and their intensity ratios actually coincide in cases of water dispersions of multichromic J-aggregates and their thin layers on a glass substrate.

A more complicated situation is observed for luminescence of the multichromic J-aggregates, in which the luminescence bands of three J-aggregates constituting a single structure are superimposed. For example, a luminescence spectrum of the single multichromic J-aggregate comprising J-aggregate of the magnesium complexes of anionic K1 dye and J-aggregates of cationic K3 and K4 dyes is shown in Fig. 10 in the case of excitation by the radiation with a wavelength λ = 405 nm. The luminescence spectrum has several bands including the bands that can be ascribed to the resonance excitonic luminescence of K1 dye ($\hbar\omega$ = 2.45 eV) and luminescence of defects (in the range $\hbar\omega$ = 1.9–2.0 eV). Both bands are shifted relative to the luminescence of monochromic J-aggregate K1 by ~0.1 eV to the low-energy side.

Two additional luminescence maxima in the ranges $\hbar\omega \approx$ 1.8 and 2.25 eV are far from the emission maxima that are specific for J-aggregates of K1 dye. Thus, it is natural to ascribe the lower-energy band to the emission of K3 dye and the band in the range $\hbar\omega \approx$ 2.25 eV to K4 dye. In each case, a short-wavelength shift by approximately 0.1 eV is observed relative to the maximum of monochromic J-aggregate. In general, the multiband luminescence spectrum of a single

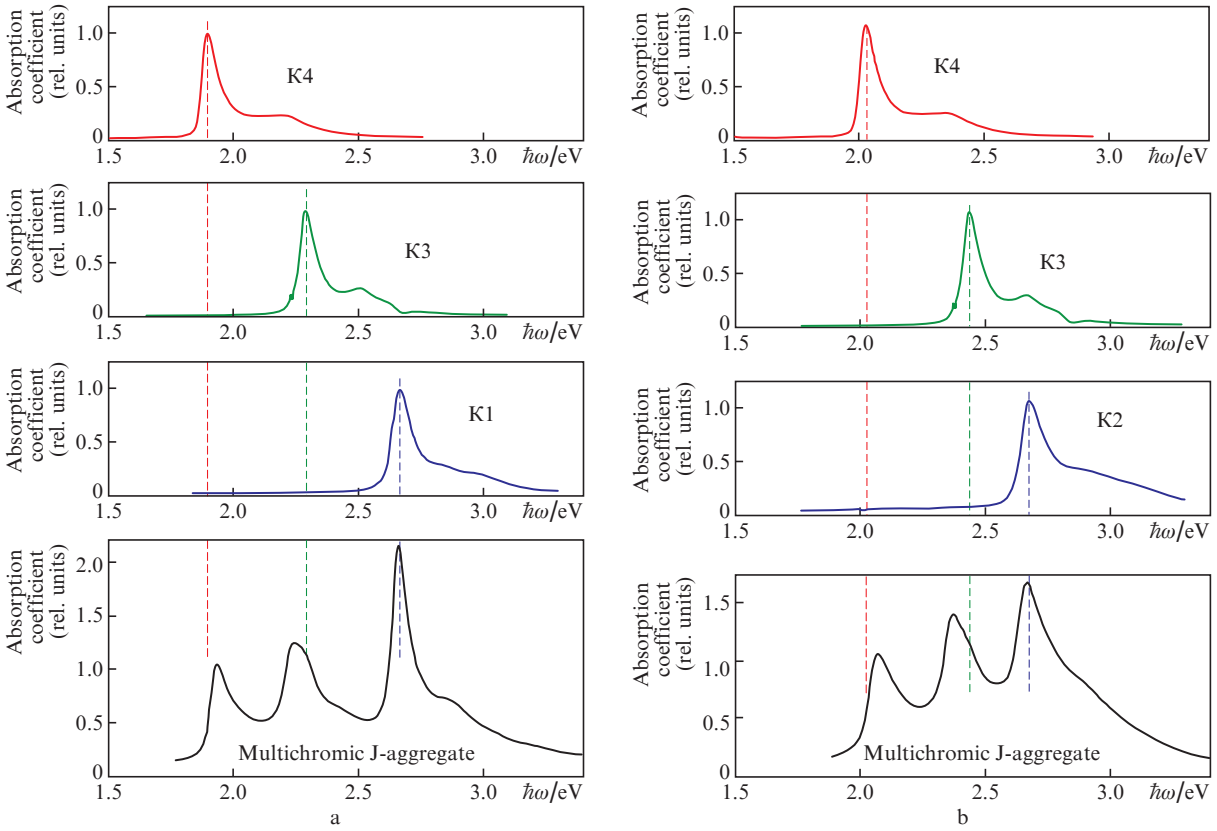

Figure 9. Photoabsorption spectra for water dispersions of multichromic J-aggregates: (a) J-aggregate of magnesium complex K1 + J-aggregate K3 + J-aggregate K4; (b) J-aggregate of magnesium complex K2 + J-aggregate K3 + J-aggregate K4. Upper curves show absorption spectra of monochromic dye J-aggregates from which the multichromic J-aggregate is combined.

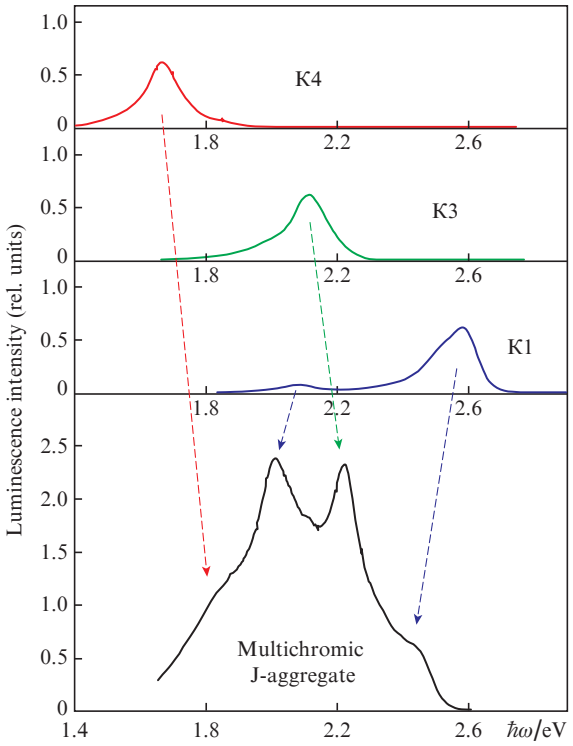

Figure 10. Luminescence spectrum of a single multichromic J-aggregate (J-aggregate of magnesium complex K1 + J-aggregate K3 + J-aggregate K4) – lower curve. Upper curves correspond to luminescence spectra of the monochromic dye J-aggregates, from which the multichromic J-aggregate is fabricated. The excitation wavelength is 405 nm ($\hbar\omega$ = 3.061 eV).

J-aggregate independently confirms the formation of a multichromic J-aggregate.

5. Organic photoelements based on multichromic dye J-aggregates

As discussed above, multiband absorption spectra of multichromic J-aggregates occupy a substantial part of the visible spectral range. This feature of multichromic J-aggregates is interesting for developing organic photoelements, whose prototypes were produced by depositing mutlichromic J-aggregates from water dispersions to an electroconducting substrate. For a transparent electrode we used a glass sample of size $50 \times 50 \times 2$ mm with a deposited electroconducting transparent ITO layer (a mixture of oxides SnO_2 and In_2O_3) possessing the surface resistivity of 7 Ω cm^{-2} (Sigma Aldrich, USA).

For obtaining a photosensitive layer, the water dispersion based on multichromic J-aggregates was centrifugated (for 15 min at 12500 rpm) and washed in bidistillate. Bidistilled water (1/8 of the initial dispersion volume) was added to the powder of J-aggregates obtained and the mixture was redispersed by ultrasound for 15 min at 40 kHz. The dispersion of J-aggregates obtained was deposited by a micro-dozer on the glass with ITO in proportion of 0.20 mL of the water dispersion of multichromic crystals per 1.0 cm^2 of substrate surface, uniformly distributed over the surface and left to dry the layer totally. Spectral characteristics of the dye layers were controlled by the spectrophotometric method. It was established that optical absorption spectra of multichromic J-aggregates of cyanine dyes at a thickness of ~0.2 μm have the optical density of about 2 in the excitonic absorption maxima. This corresponds to the absorption coefficient of more than ~ 10^5 cm^{-1}, which is by an order of magnitude greater than in silicon. It makes thin layers of J-aggregates of cyanine dyes especially promising for developing thin-film organic photoelements possessing a high photosensitive area. Above the dye layer, a layer of poly-N-9-vinylcarbazole [PVC, the molar mass is 5×10^4 (Sigma Aldrich)] was deposited, which served as a hole-transporting layer. The PVC layer was deposited from the solution with a concentration of 2.5×10^{-4} M (recalculated to a PVC monomer) in carbon tetrachloride. The PVC solution was deposited by using a micro-dozer in proportion of 1.0 mL per 5.0 cm^2 of the ITO-electrode surface. Then the layer was dried at room temperature. Above the PVC layer, an electroconducting contact layer of thickness 0.2 mm was deposited by using a paste with silver microparticles. Then, this layer was sealed from external action by an aluminium foil with an adhesion layer.

The structure of a photosensitive nano-architecture of the organic photoelement based on multilayer J-aggregates of three dyes is shown in Fig. 11.

Figure 12 presents an electrical circuit for connecting the organic photoelement shown in Fig. 11. The main parts of the installation for measuring photoelectric properties of organic photoelement are: a transimpedance amplifier (a current–voltage converter) with a commutated set of calibrated load resistors in the range of 1–100 MΩ, which provided measurements of the voltage drop; a complete measurement toolkit

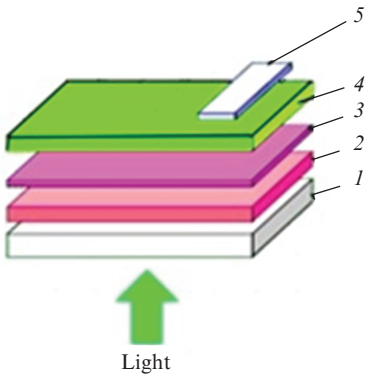

Figure 11. Structure of an organic photoelement: (*1*) glass substrate; (*2*) transparent ITO-electrode (anode); (*3*) photosensitive crystal layer of multichromic multilayer dye J-aggregates (the layer thickness is ~0.2 μm); (*4*) polyvinylcarbazole layer; (*5*) silver electrode (metal cathode).

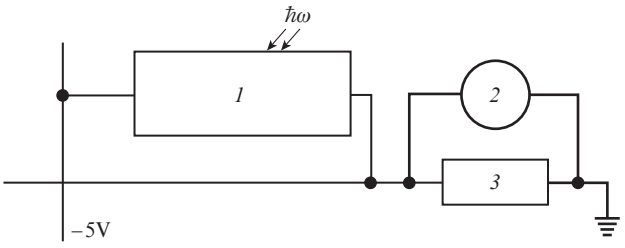

Figure 12. Electrical circuit for the organic photoelement: (*1*) organic photoelement; (*2*) voltmeter; (*3*) load resistor; the external voltage shift is –5V.

for working with electrical schemes (Digilent Analog Discovery 2, USA) comprising a double-channel oscilloscope and a pulse oscillator; and a set of light-emitting diodes in the blue, green, and red spectral ranges. Rectangular voltage pulses were applied to the organic photoelement. The voltage varied in the range of 0–5 V. The light sources were light-emitting diodes produced by Hüey Jann Electronics Industries Co. (Taiwan): blue (HPR40E-48K100BI), green (HPR40E-43K100GA), and red (HPR40E-45K100RB).

Under exposure (illumination), the total electric current I_{sum} through the photoelement and a load resistor is the sum of two main components: the dark current I_d and photocurrent response I_{pc}:

$$I_{sum} = I_d + I_{pc}. \quad (1)$$

A value of the photocurrent response was found from (1). The dark electrical conductivity and photoconductivity were measured at a standard value of the voltage bias –5 V (applied from the side of the metal electrode) and calibrated load resistor of 1.00 MΩ. A silicon photodiode Vishay BPW34 was used as a reference standard photodiode with known quantum efficiency of light energy conversion and for measuring the light power passing onto the photoelement. Photoelectric characteristics were measured at a temperature of 20 °C.

The external quantum efficiency η (the ratio of the number of detected charge carries to the number of photons entering the light sensitive area, expressed as a percentage) of developed organic photodiodes based on multichromic J-aggregates is expressed by the formula [68]

$$\eta = \frac{(Sj_{pc}/e)}{(P/\hbar\omega)} \times 100\% = \frac{2\pi\hbar c S j_{pc}}{e\lambda P} \times 100\%, \quad (2)$$

where j_{pc} is the density of the photocurrent I_{pc} through a light sensitive area S of the photoelement; λ and $\hbar\omega$ are the wavelength and energy of the exposure light quantum, respectively; P is the light power incident onto the sample; e is the elementary electric charge; c is the speed of light in vacuum; and $\hbar$ is Planck's constant.

Results of photoelectric measurements of the dark electric conductivity, photocurrent, and quantum efficiency of photoconductivity are presented in Table 2. One can see that the dark current density in the layers based on synthesised structures is at a level of 0.1 μA cm^{-2}, the quantum efficiency of photoconduction in the experimental conditions is 2.7%–6.1% (depending on the kind of dye in the J-aggregate). Thus, one may conclude that each of the three J-aggregates comprised in the multichromic crystal demonstrates an independent and substantial response under irradiation in the excitonic absorption maxima.

6. Conclusions

Photophysical properties of synthesised multichromic J-aggregates of dyes absorbing light in a wide spectral range have been studied. These molecular ensembles have been produced by using the method of matrix synthesis of J-aggregates of cationic cyanine dyes on a surface of a negatively charged platform of J-aggregates of magnesium complexes of anionic dyes. It is shown that the devices have intensive excitonic J-bands of optical absorption in the visible and IR spectral ranges.

It has been established that multichromic J-aggregates based on three cyanine dyes of various structure are efficient photosensitive organic semiconductors and provide an efficient photo-response both in the maximum of J-band absorption of the anionic metal-complex platform and in the maxima of two absorption bands of J-aggregates of cationic dyes. Thus, we may conclude that the controlled crystallisation and matrix synthesis of aggregates of cyanine dyes open the way to technology for producing nano-size and micro-size semiconductor highly ordered organic molecular crystals of prescribed size, which possess wide spectra of luminescence and sensitivity to radiation.

Multichromic J-aggregates of dyes can be employed for developing thin-film photo-switches and light emitting devices with tunable radiation frequency. Due to three intensive absorption bands they also have a series of advantages for producing on this basis hybrid metal-organic nanostructures with controlled optical properties as compared to earlier employed monochromic J- and H-aggregates of a series of cyanine dyes.

Thus, multilayer multichromic molecular aggregates of dyes synthesised in the present work are promising for the employment as the element basis for organic and hybrid organo/inorganic optoelectronics and photonics, including optoelectronic nano-devices on this base functioning on new principles.

Acknowledgements. The work was supported by the Russian Science Foundation (Project No. 14-22-00273-P). Authors are

Table 2. Spectral and photoelectric characteristics of layers of multichromic dye J-aggregates.

Type of dye in J-aggregate	Position of excitonic absorption maximum /nm	Optical density of layer	Dark current density /μA cm^{-2}	Photocurrent density /μA cm^{-2}	Quantum efficiency of photoconductivity (%)
Multichromic J-aggregate Magnesium complex of J-aggregate K1 + J-aggregate K3 + J-aggregate K4					
K1	465	2.2	0.10	5.2	5.8
K3	545	1.8		4.1	3.9
K4	650	1.3		3.4	2.7
Multichromic J-aggregate Magnesium complex of J-aggregate K2 + J-aggregate K3 + J-aggregate K4					
K2	492	2.4	0.11	5.7	6.1
K3	545	2.1		4.2	4.0
K4	650	1.4		3.6	2.9

grateful to A.I. Tolmachev and Yu.L. Slominskii (IOC NAS Ukraine, Kiev) for synthesising dye K2, V.I. Pogonin (GEOChI RAS) and B.V. Pokid'ko (MIREA) for help in experiments, and M.V. Kochiev (LPI) for photoluminescence kinetic measurements.

Appendix

Solutions were prepared by using deionized bidistilled water with a resistivity of 18 MΩ cm subjected to UV irradiation and reverse osmosis cleaning by employing a Millipore Milli-Q3 Direct UV water cleaning unit (France). Dye and metal salt batches were weighted on a GR-202 A&D electronic microanalytic balance (Japan). The electrokinetic potential of particles of dye magnesium complexes in dispersions was determined by using a Zetasizer Nano ZS (Malvern, Great Britain) device. The measurements were taken at 25 °C with the employment of a polystyrene cell and submersible electrode at the potential applied of 10 V.

Magnesium complexes of dyes were synthesised by using magnesium sulphate ($MgSO_4$) of 'Chemically Purity'. Multichromic cationic-anionic J-aggregates were synthesised by the method described in [52, 53] using a magnetic stirrer with varied speed of rotation (Ekoniks-Ekspert 'RITM-01', Russia). At each stage of synthesis, the mixing lasted for 10 min at the rotation speed of 600 rpm. The synthesis temperature was $T = 22$ °C.

As an example, below we present the method for synthesising the multilayer cationic-anionic J-aggregate which includes magnesium complexes of K1 dye as the anionic platform and J-aggregates of cationic K3 and K4 dyes assembled on its surface.

At a first stage, the platform of magnesium complexes of anionic dyes was synthesised. For this purpose, 90 mL of water solution of K1 dye with a concentration of 5.0×10^{-5} M was prepared in a beaker. Then, 10 mL of magnesium sulphate solution with a concentration of 10^{-3} M was added and the solution was mixed by a magnetic stirrer. The formation of J-aggregates of magnesium complexes of K1 dye was controlled with the spectrophotometric method by a reduction of the optical density in the maxima of absorption bands of K1 dye monomers and dimers at λ = 428 and 408 nm, respectively, and by an increase of excitonic absorption maximum of K1 dye J-aggregates at λ = 465 nm.

At a second stage, for obtaining multichromic J-aggregates, 5.0 mL of the solution of cationic K3 dye with a concentration of 5.0×10^{-4} M in ethanol (96%) was added to the dispersion of J-aggregates of magnesium complexes of K1 dye. The mixture obtained was mixed for 10 min and 5.0 mL of the solution of cationic K4 dye with a concentration of 5.0×10^{-4} M in ethanol (96%) was added. Then the mixture was mixed again for 10 min. At each stage, the formation of the layers of J-aggregates of cationic dyes on a surface of anionic platform of K1 dye was controlled by absorption spectra.

Multichromic structures based on anionic platform of magnesium complexes of K2 dye were synthesised in a similar way.

References

1. Shirasaki Y., Supran G.J., Bawendi M.G., Bulović V. *Nature Photon.*, **7**, 13 (2013).
2. Pushkarev A.P., Bochkarev M.N. *Usp. Khim.*, **85**, 1338 (2016).
3. Stratakis E., Kymakis E. *Materials Today*, **16**, 133 (2013).
4. Milichko V.A., Shalin A.S., Mukhin I.S., Kovrov A.E., Krasilin A.A., Vinogradov A.V., Belov P.A., Simovskii S.R. *Phys. Usp.*, **59**, 727 (2016) [*Usp. Fiz. Nauk*, **186**, 801 (2016)].
5. Wang S., Wang X.-W., Li B., Chen H.-Z., Wang Y.-L., Dai L., Oulton R.F., Ma R.-M. *Nature Commun.*, **8**, 1889 (2017).
6. Wang Z., Meng X., Kildishev A.V., Boltasseva A., Shalaev V.M. *Laser Photon. Rev.*, **11**, 1700212 (2017).
7. Kuznetsova T.I., Lebedev V.S. *Phys. Rev. E*, **78**, 016607 (2008).
8. Chen Z.-X., Wu Z.-J., Ming Y., Zhang X.-J., Lu Y.-Q. *AIP Adv.*, **4**, 017103 (2014).
9. Kuznetsova T.I., Lebedev V.S. *Quantum Electron.*, **32**, 727 (2002) [*Kvantovaya Elektron.*, **32**, 727 (2002)].
10. Kuznetsova T.I., Lebedev V.S., Tsvelik A.M. *J. Opt. A: Pure Appl. Opt.*, **6**, 338 (2004).
11. Kuznetsova T.I., Lebedev V.S. *JETP Lett.*, **79**, 62 (2004) [*Pis'ma Zh. Exp. Teor. Fiz.*, **79**, 70 (2004)].
12. Kuznetsova T.I., Lebedev V.S. *Phys. Rev. B*, **70**, 035107 (2004).
13. Gramotnev D.K., Bozhevolnyi S.I. *Nature Photon.*, **8**, 13 (2014).
14. Kazantsev D.V., Kuznetsov E.V., Timofeev S.V., Shelaev A.V., Kazantseva E.A. *Phys. Usp.*, **60**, 259 (2017) [*Usp. Fiz. Nauk*, **187**, 277 (2017)].
15. Vashchenko A.A., Lebedev V.S., Vitukhnovskii A.G., Vasiliev R.B., Samatov I.G. *JETP Lett.*, **96**, 113 (2012) [*Pis'ma Zh. Exp. Teor. Fiz.*, **96**, 118 (2012)].
16. Vashchenko A.A., Vitukhnovskii A.G., Lebedev V.S., Selyukov A.S., Vasiliev R.B., Sokolikova M.S. *JETP Lett.*, **100**, 86 (2014) [*Pis'ma Zh. Exp. Teor. Fiz.*, **100**, 94 (2014)].
17. Vitukhnovsky A.G., Lebedev V.S., Selyukov A.S., Vashchenko A.A., Vasiliev R.D., Sokolikova M.C. *Chem. Phys. Lett.*, **619**, 185 (2015).
18. Selyukov A.S., Vitukhnovskii A.G., Lebedev V.S., Vashchenko A.A., Vasiliev R.B., Sokolikova M.S. *JETP*, **120**, 595 (2015) [*Zh. Exp. Teor. Fiz.*, **147**, 687 (2015)].
19. Stratakis E., Kymakis E. *Materials Today*, **16** (4) 133 (2013).
20. Cheng P., Li G., Zhan X., Yang Y. *Nature Photon.*, **12**, 131 (2018).
21. Lunt R.R., Bulović V. *Appl. Phys. Lett.*, **98**, 1133051 (2011).
22. Osedach T.P., Lacchetti A., Lunt R.R., Andrew T.L., Brown P.R., Akselrod G.M., Bulović V. *Appl. Phys. Lett.*, **101**, 113303 (2012).
23. Wang F., Lu C.H., Willner I. *Chem. Rev.*, **114**, 2881 (2014).
24. Shapiro B.I. *Usp. Khim.*, **75**, 484 (2006).
25. Kobayashi T. (Ed.) *J-Aggregates* (New Jersey: World Scientific, 2012) Vol. 2.
26. Würthner F., Kaiser T.E., Saha-Möller C.R. *Angew. Chem. Int. Ed.*, **50**, 3376 (2011).
27. James T.H. The *Theory of the Photographic Process* (New York: Macmillan, 1977; Leningrad: Khimiya, 1980).
28. Shapiro B.I. *Teoreticheskie nachala fotograficheskogo protsessa* (Theoretical Principles of the Photographic Process) (Moscow: EditorialURSS, 2000).
29. Kometani N., Tsubonishi M., Fujita T., Asami K., Yonezawa Y. *Langmuir*, **17**, 578 (2001).
30. Wiederrecht G.P., Wurtz G.A., Bouhelier A. *Chem. Phys. Lett.*, **461**, 171 (2008).
31. Lebedev V.S., Vitukhnovsky A.G., Yoshida A., Kometani N., Yonezawa Y. *Colloids Surf. A: Physicochem. Eng. Aspects.*, **326**, 204 (2008).
32. Lebedev V.S., Medvedev A.S., Vasil'ev D.N., Chubich D.A., Vitukhnovskii A.G. *Quantum Electron.*, **40**, 246 (2010) [*Kvantovaya Elektron.*, **40**, 246 (2010)].
33. Shapiro B.I., Kol'tsova E.S., Vitukhnovskii A.G., Slominskyy Yu.L. *Ross. Nanotekhnol.*, **6**, 5 (2011).
34. Vujačić A., Vasić V., Dramićanin M., Sovilj S.P., Nataša Bibić N., Hranisavljevic J., Wiederrecht G.P. *J. Phys. Chem. C*, **116**, 4655 (2012).
35. Laban B.B., Vodnik V., Vasić V. *Nanospectroscopy*, **1**, 54 (2015).
36. Lebedev V.S., Medvedev A.S. *Quantum Electron.*, **42**, 701 (2012) [*Kvantovaya Elektron.*, **42**, 701 (2012)].
37. Lebedev V.S., Medvedev A.S. *J. Russ. Laser Res.*, **34**, 303 (2013).
38. Antosiewicz T.J., Apell S.P., Shegai T. *ACS Photonics*, **1**, 454 (2014).
39. Yoshida A., Kometani N. *J. Phys. Chem. C*, **114**, 2867 (2010).
40. Lebedev V.S., Medvedev A.S. *Quantum Electron.*, **43**, 1065 (2013) [*Kvantovaya Elektron.*, **43**, 1065 (2013)].
41. Gülen D. *J. Phys. Chem. B*, **117**, 11220 (2013).

42. Kondorskiy A.D., Kislov K.S., Lam N.T., Lebedev V.S. *J. Russ. Laser Res.*, **36**, 175 (2015).
43. Yoshida A., Uchida N., Kometani N. *Langmuir*, **25**, 11802 (2009).
44. Ni W., Ambjörnsson T., Apell S.P., Chen H., Wang J. *Nano Lett.*, **10**, 77 (2010).
45. Zengin G., Johansson G., Johansson P., Antosiewicz T.J., Käll M., Shegai T. *Scientific Reports*, **3**, 3074 (2013).
46. Melnikau D., Savateeva D., Susha A., Rogach A.L., Rakovich Y.P. *Nanoscale Res. Lett.*, **8**, 134 (2013).
47. Shapiro B.I., Tyshkunova E.S., Kondorskiy A.D., Lebedev V.S. *Quantum Electron.*, **45**, 1153 (2015) [*Kvantovaya Elektron.*, **45**, 1153 (2015)].
48. Slavnova T.D., Chibisov A.K., Görner H. *J. Phys. Chem. A*, **109**, 4758 (2005).
49. Shapiro B.I., Belonozhkina E.A., Tyapina O.A., Kuz'min V.A. *Ross. Nanotekhnol.*, **5**, 67 (2010).
50. Shapiro B.I. *Ross. Nanotekhnol.*, **3**, 72 (2008).
51. Nekrasov A.D., Shapiro B.I. *Khim. Vys. Ener.*, **45**, 162 (2011).
52. Shapiro B.I., Satalkina E.A., Nekrasov A.D. *Ross. Nanotekhnol.*, **9**, 8 (2014).
53. Shapiro B.I., Manulik E.V. *Ross. Nanotekhnol.*, **11**, 14 (2016).
54. Shapiro B.I., Manulik E.V., Prokhorov V.V. *Ross. Nanotekhnol.*, **11**, 10 (2016).
55. Hiroshi Y. *Ann. Rep. Progr. Chem., Sect. C*, **100**, 99 (2004).
56. Kometani N., Nakajima H., Asami K., Yonezawa Y., Scheblykin I.G., Vitukhnovsky A.G. *J. Luminesc.*, **87-89**, 770 (2000).
57. Malyukin Yu.V., Seminozhenko V.P., Tovmachenko O.G. *JETP*, **80**, 460 (1995) [*Zh. Exp. Teor. Fiz.*, **107**, 812 (1995)].
58. Markov R.V., Plekhanov A.I., Ivanova Z.M., Orlova N.A., Shelkovnikov V.V., Ivanov A.A., Alfimov M.V. *JETP*, **99**, 480 (2004) [*Zh. Exp. Teor. Fiz.*, **126**, 549 (2004)].
59. Sorokin A.V., Pereverzev N.V., Grankina I.I., Yefimova S.L., Malyukin Yu.V. *J. Phys. Chem. C*, **119**, 27865 (2015).
60. Yefimova S.L., Sorokin A.V., Katrunov I.K., Malyukin Yu.V. *Low Temp. Phys.*, **37**, 157 (2011).
61. Gierschner J., Park S.Y. *J. Mater. Chem. C*, **1**, 5818 (2013).
62. Merdasa A., Jiménez A.J., Camacho R., Matthias M., Würthner F., Scheblykin I.G. *Nano Lett.*, **14**, 6774 (2014).
63. Malyukin Yu. *Phys. Stat. Sol. (C)*, **3**, 3386 (2006).
64. Dimitriev O.P., Piryatinski Y.P., Slominskii Y.L. *J. Phys. Chem. Lett.*, **9**, 2138 (2018).
65. Bricks J.L., Slominskii Y.L., Panas I.D., Demchenko A.P. *Methods Appl. Fluoresc.*, **21**, 01200 (2017).
66. Hestand N.J., Spano F.C. *Chem. Rev*., **118**, 7069 (2018).
67. Anantharaman S.B., Yakunin S., Peng C. *J. Phys. Chem. C*, **121**, 958 (2017).
68. Davidenko N.A., Ishchenko A.A., Pavlov V.A. *Zh. Nauchn. Prikl. Fotogr.*, **44**, 52 (1999).